

Green's Identity Formula and its Application to Water Wave  
Boundary-Value Problems

by

Takeshi IJIMA\*, Chung Ren CHOU\*\* and Akinori YOSHIDA\*\*

Abstract

Green's function is one of the most powerful tools to analyze the boundary-value problems on water wave motion. However, in many cases, it is difficult to derive the Green's function satisfying the imposed boundary conditions of the problems. This paper shows an extremely simple method of analyses by the direct use of Green's identity formula instead of Green's function. The proposed method can be applied to the two-dimensional boundary-value problems of small amplitude waves, including fixed or oscillating boundaries and impermeable or permeable boundaries. In this paper, the formulations and numerical calculations are introduced for several examples.

I Introduction

The problems on wave reflection and transmission at permeable breakwater and seawall with vertical faces and the motion of floating body with rectangular cross-section etc. are the boundary-value problems for the fluid regions with vertical and horizontal linear boundary lines and one of the author has shown (1971, 1972) that such a problem can be analyzed by the method of continuation of velocity potentials between adjacent fluid regions. However, the boundary-value problems for fluid regions with arbitrary shapes such as permeable structures with sloped faces, floating bodies with arbitrary cross-sections and so on cannot be solved by above method and frequently even by the use of Green's function.

The method to be introduced in this paper is not to use Green's function but to use logarithmic function of the distance between the point on the boundary and the inner point of fluid region in the Green's theorem. By means of our method, the problems concerning to the sloped-face permeable structures, the floating body in variable water depth area and so on are easily formulated and numerically analyzed. In the followings, the formulations and numerical calculations for small amplitude waves are introduced and compared with experimental results.

II Green's Theorem and Identity Formula

We assume that a potential function  $\phi(x, z)$  is defined in a closed domain enclosed by a curve  $D$  in  $x, z$ -plane as shown in Fig.2-1. Indicating the point on the boundary curve  $D$  by  $(\xi, \eta)$ , the outward normal by  $\nu$ , the distance between the point  $(\xi, \eta)$  and a point  $(x, z)$  in the domain by  $r$ , that is,  $r = \sqrt{(\xi - x)^2 + (\eta - z)^2}$ , and the constant reference length to the geometrical size of the domain by  $h_0$ , it

\* Professor: Faculty of Engineering, Kyushu University, Fukuoka, JAPAN

\*\* Master of Engineering, Graduate Student at the Kyushu University

follows by Green's theorem that the potential value at point  $(x, z)$  is provided by the potential values  $\phi(\xi, \eta)$  and its normal derivatives  $\partial\phi(\xi, \eta)/\partial(\nu/h_0)$  on the boundary curve as follows:

$$\phi(x, z) = \frac{1}{2\pi} \int_D \left[ \phi(\xi, \eta) \frac{\partial \log(R/h_0)}{\partial(\nu/h_0)} - \frac{\partial\phi(\xi, \eta)}{\partial(\nu/h_0)} \log(R/h_0) \right] \frac{dS}{h_0} \quad (2.1)$$

If the point  $(x, z)$  lies on the boundary at  $(\xi', \eta')$ , Eq.(2.1) leads to the Green's identity formula as follows:

$$\phi(\xi', \eta') = \frac{1}{\pi} \int_D \left[ \phi(\xi, \eta) \frac{\partial \log(R/h_0)}{\partial(\nu/h_0)} - \frac{\partial\phi(\xi, \eta)}{\partial(\nu/h_0)} \log(R/h_0) \right] \frac{dS}{h_0} \quad (2.2)$$

where

$$R = \sqrt{(\xi - \xi')^2 + (\eta - \eta')^2}$$

In Eq.(2.1) and (2.2), the integration denotes the line integral along the curve  $D$ . Then, dividing the boundary curve into  $N$  small elements by  $N$  points and indicating the length and central point of the  $j$ -th element as  $\Delta S_j$  and  $(\xi_j, \eta_j)$  as shown by Fig.2-2, Eq.(2.1) and (2.2) are approximated by the following summation equations, respectively.

$$\phi(x, z) = \frac{1}{2} \sum_{j=1}^N [\bar{E}_{xj} \phi(j) - E_{xj} \bar{\phi}(j)] \quad (2.3)$$

$$\phi(i) = \sum_{j=1}^N [\bar{E}_{ij} \phi(j) - E_{ij} \bar{\phi}(j)] \quad (2.4)$$

where

$$\phi(j) = \phi(\xi_j, \eta_j), \quad \bar{\phi}(j) = \partial\phi(\xi_j, \eta_j)/\partial(\nu/h_0) \quad (2.5)$$

$$E_{xj} = \frac{1}{\pi} \int_{\Delta S_j} \log\left(\frac{r_{xj}}{h_0}\right) \frac{dS}{h_0}, \quad \bar{E}_{xj} = \frac{1}{\pi} \int_{\Delta S_j} \frac{\partial}{\partial(\nu/h_0)} \log\left(\frac{r_{xj}}{h_0}\right) \frac{dS}{h_0} \quad (2.6)$$

$$E_{ij} = \frac{1}{\pi} \int_{\Delta S_j} \log\left(\frac{R_{ij}}{h_0}\right) \frac{dS}{h_0}, \quad \bar{E}_{ij} = \frac{1}{\pi} \int_{\Delta S_j} \frac{\partial}{\partial(\nu/h_0)} \log\left(\frac{R_{ij}}{h_0}\right) \frac{dS}{h_0}$$

$E_{xj}$ ,  $\bar{E}_{xj}$  and  $E_{ij}$ ,  $\bar{E}_{ij}$  are integrated values over the  $j$ -th element referring to the point  $x = (x, z)$  and  $i = (\xi_i, \eta_i)$ , respectively, and they are calculated numerically as follows:

$$E_{ij} = \frac{1}{\pi} \log\left(\frac{R_{ij}}{h_0}\right) \frac{\Delta S_j}{h_0}, \quad E_{ii} = \frac{1}{\pi} \left( \log \frac{\Delta S_i}{2h_0} - 1 \right) \frac{\Delta S_i}{h_0} \quad (2.7)$$

$$\bar{E}_{ij} = \theta_{ij}/\pi, \quad \bar{E}_{ii} = 0$$

where  $\theta_{ij}$  is the subtending angle of the point  $i = (\xi_i, \eta_i)$  to the  $j$ -th element, and

$$R_{ij} = \sqrt{(\xi_j - \xi_i)^2 + (\eta_j - \eta_i)^2}, \quad \Delta S_j = \sqrt{(\Delta \xi_j)^2 + (\Delta \eta_j)^2}$$

$$\Delta \xi_j = \frac{1}{2} (\xi_{j+1} - \xi_{j-1}), \quad \Delta \eta_j = \frac{1}{2} (\eta_{j+1} - \eta_{j-1})$$

$E_{xj}$  and  $\bar{E}_{xj}$  are calculated, replacing the point  $i = (\xi_i, \eta_i)$  by  $x = (x, z)$  in Eq. (2.7).

Eq. (2.1) or (2.3), the Green's theorem, states that the potential function at any point in the domain is determined by its boundary-values and normal derivatives of the interested potential function.

Eq. (2.2) or (2.4), the Green's identity formula, states that the boundary-values  $\phi(\xi, \eta)$  and its normal derivatives  $\bar{\phi}(\xi, \eta)$  are in linear relationships which are defined by the geometrical shape of the domain. This is the first set of relations between  $\phi$  and  $\bar{\phi}$  on the boundary.

Therefore, if another set of relations between  $\phi$  and  $\bar{\phi}$  is provided, it follows that they should be determined by solving the two set of relations, simultaneously. And, in our problems, the second relation is demonstrated by dynamical or kinematical boundary conditions on the boundaries of the interested domain.

### III Wave Transformation by Permeable Seawall and Breakwater

As the first example, we consider the wave reflection and transmission at permeable breakwater with sloped faces. In Fig.3-1, we take the origin O of the coordinate system at still water surface, x- and z-axis in horizontal and vertically upwards. CDD'C' is assumed to be the permeable breakwater with uniform porosity V on the sea bed of variable water depth, where the depth at sufficiently distant from the breakwater is constant h to the right and h' to the left. The incident wave of frequency  $\sigma$  and amplitude  $\zeta_0$  is assumed to come from the right. We take the geometrical boundaries AB and A'B' at  $x = \ell$  and  $-\ell'$ , where the depths are h and h', respectively and divide the fluid region into four parts (O) (I) (II) (III) and (O') as shown in the figure.

The fluid motion in regions (O) (I) (III) and (O') is assumed to have velocity potential  $\bar{\Phi}(x, z; t)$  with potential function  $\phi(x, z)$  as follows:

$$\bar{\Phi}(x, z; t) = \frac{g \zeta_0}{\rho} \phi(x, z) e^{i\sigma t} \quad (3.1)$$

where g is the gravity acceleration and t is time. The potential functions in regions (O) (I) (III) and (O') are denoted by  $\phi_0(x, z)$ ,  $\phi^{(1)}(x, z)$ ,  $\phi^{(3)}(x, z)$  and  $\phi_0'(x, z)$ , respectively.

(i) Since the fluid regions (O) and (O') are of constant depth and so far from the breakwater that the scattering waves are damped to be vanished, the potential functions for them are demonstrated simply by Eq. (3.2) and (3.3) without scattering terms.

$$\phi_0(x, z) = [e^{ik(x-l)} + \psi e^{-ik(x-l)}] \cdot A(kz) \quad (3.2)$$

$$\phi_0'(x, z) = \psi' e^{-ik'(x+l')} \cdot A(k'z) \quad (3.3)$$

In Eq. (3.2), the first term is for the incident wave and the second term is for the reflected wave with complex reflection coefficient  $\psi$ . Eq. (3.3) is for the transmitted wave with complex transmission coefficient  $\psi'$ . The functions  $A(kz)$  and  $A'(k'z)$  are given by Eq. (3.4) with wave number  $k$  and  $k'$  for regions (O) and (O'), which are determined by Eq. (3.5). The reflection and transmission coefficients  $K_r$  and  $K_t$  are provided by Eq. (3.6).

$$A(kz) = \frac{\cosh k(z+h)}{\cosh kh}, \quad A(k'z) = \frac{\cosh k'(z+h')}{\cosh k'h'} \quad (3.4)$$

$$kh \tanh kh = \frac{\rho^2 h}{g}, \quad k'h' \tanh k'h' = \frac{\rho^2 h'}{g} \quad (3.5)$$

$$K_r = |\psi|, \quad K_t = |\psi'| \quad (3.6)$$

(ii) The fluid regions (I) and (III) have potential functions  $\phi^{(1)}(x, z)$  and  $\phi^{(3)}(x, z)$ , respectively. And, on the free surface AC and C'A' at  $z = 0$ , the free surface boundary condition provides the following relations.

$$\frac{\partial \phi^{(1),(3)}}{\partial z} = \frac{\rho^2}{g} \phi^{(1),(3)} \quad \text{or} \quad \bar{\phi}^{(1),(3)} = \frac{\partial \phi^{(1),(3)}}{\partial (z/h_0)} = \Gamma \phi^{(1),(3)} \quad \text{where} \quad \Gamma = \frac{\rho^2 h_0}{g} \quad (3.7)$$

and  $h_0$  is taken as the distance between point A and B'.

On the geometrical boundaries AB ( $x = l$ ) and A'B' ( $x = -l'$ ), we have from Eq. (3.2) and (3.3)

$$\phi_0 = (1 + \psi) \cdot A(kz), \quad \bar{\phi}_0 = h_0 \frac{\partial \phi_0}{\partial x} = i \lambda_0 (1 - \psi) A(kz) \quad (3.8)$$

$$\phi_0' = \psi' \cdot A(k'z), \quad \bar{\phi}_0' = -h_0 \frac{\partial \phi_0'}{\partial x} = -i \lambda_0' \psi' A(k'z) \quad (3.9)$$

where  $\lambda_0 = kh_0, \quad \lambda_0' = k'h_0 \quad (3.10)$

On impervious bottom DB and D'B', we have

$$\bar{\phi}^{(1),(3)} = \partial \phi^{(1),(3)} / \partial (z/h_0) = 0 \quad (3.11)$$

(iii) As for the permeable region (II), indicating the quantities for fluid motion by superscript \*, the mass and momentum equations are demonstrated by horizontal and vertical macroscopic fluid velocities  $u^*$ ,  $w^*$  and fluid pressure  $p^*$  as follows:

$$\frac{\partial u^*}{\partial x} + \frac{\partial w^*}{\partial z} = 0$$

$$\frac{1}{V} \frac{\partial u^*}{\partial t} = -\frac{1}{\rho} \frac{\partial p^*}{\partial x} - \frac{\mu}{V} u^*, \quad \frac{1}{V} \frac{\partial w^*}{\partial t} = -\frac{1}{\rho} \frac{\partial p^*}{\partial z} - \frac{\mu}{V} w^* - g \quad (3.12)$$

where  $\rho$  is the fluid density,  $V$  is the porosity of the breakwater,  $\mu$  is the linearized coefficient of drag force to the porous material induced by the fluid flow through the breakwater. The fluid motion of Eq.(3.12) has velocity potential  $\Phi^*(x,z;t)$ , which is expressed by Eq.(3.13) with potential function  $\phi^*(x,z)$ , and fluid velocities, pressure and surface profile are provided by Eq.(3.13) (3.14),

$$\Phi^*(x,z;t) = \frac{\eta \zeta_0}{\rho} \phi^*(x,z) e^{i\sigma t} \quad (3.13)$$

$$u^* = \partial \Phi^* / \partial x, \quad w^* = \partial \Phi^* / \partial z, \quad p^* / \rho g \zeta_0 = -i\beta \phi^*(x,z) e^{i\sigma t}$$

$$\zeta^* / \zeta_0 = -i\beta \phi^*(x,z) e^{i\sigma t}, \quad \beta = \frac{\alpha}{V}, \quad \alpha = 1 + i\mu/\sigma \quad (3.14)$$

On the free surface  $CC'$ , we have Eq.(3.15) and on the impervious bottom  $DD'$ , we have Eq.(3.16).

$$\frac{\partial \phi^*}{\partial z} = \alpha \frac{\partial^2}{\partial x^2} \phi^* \quad \bar{\phi}^* = \alpha \Gamma \phi^* \quad (3.15)$$

$$\frac{\partial \phi^*}{\partial v} = 0 \quad \bar{\phi}^* = 0 \quad (3.16)$$

(iv) On the boundary surface  $CD$  and  $C'D'$  between fluid region (I) and (II), and (II) and (III), it follows from the continuity conditions of mass and energy flux through the boundaries that

$$\bar{\phi}^* = h_0 \frac{\partial \phi^*}{\partial v} = h_0 \frac{\partial \phi^{(1)}}{\partial v} = \bar{\phi}^{(1)}, \quad \phi^* = \frac{1}{\beta} \phi^{(1)} \quad \text{on } CD \quad (3.17)$$

$$\bar{\phi}^* = \bar{\phi}^{(3)}, \quad \phi^* = \frac{1}{\beta} \phi^{(3)} \quad \text{on } C'D' \quad (3.18)$$

(v) As shown in Fig.3-2, denoting the potential functions on the boundaries  $AC$ ,  $CD$ ,  $DB$  and  $BA$  for fluid region (I) by  $\phi_1^{(1)}$ ,  $\phi_2^{(1)}$ ,  $\phi_3^{(1)}$  and  $\phi_0$ , on the boundaries  $C'C$ ,  $CD$ ,  $DD'$  and  $D'C'$  for fluid region (II) by  $\phi_1^*$ ,  $\phi_2^*$ ,  $\phi_3^*$  and  $\phi_4^*$ , and on the boundaries  $C'A'$ ,  $A'B'$ ,  $B'D'$  and  $D'C'$  for fluid region (III) by  $\phi_1^{(3)}$ ,

$\phi_0^{(1)}, \phi_2^{(2)}, \phi_3^{(3)}$ , dividing these boundaries into  $N_1^{(1)}, N_2^{(1)}, N_3^{(1)}$ ,  $M$  elements;  $N_1^*, N_2^*, N_3^*$  elements and  $N_1^{(3)}, M', N_2^{(3)}, N_3^{(3)}$  elements, respectively and taking the outward normal for regions (I) and (III) and inward normal for region (II), and applying the boundary conditions (3.7) (3.8) (3.9) (3.11) to the Green's identity formula (2.4) for regions (I) and (III) and conditions (3.15) (3.16) (3.17) (3.18) to the Eq. (2.4) for region (II), we have the following equations:

(a) For fluid region (I):

$$\begin{aligned}
 & -\phi^{(1)}(i) + \sum_{j=1}^{N_1^{(1)}} (\bar{E}_{ij} - \Gamma E_{ij}) \phi_i^{(1)}(j) + \sum_{j=1}^{N_2^{(1)}} [\bar{E}_{ij} \phi_2^{(1)}(j) - E_{ij} \bar{\phi}_2^{(1)}(j)] \\
 & + \sum_{j=1}^{N_3^{(1)}} \bar{E}_{ij} \phi_3^{(1)}(j) + \psi \sum_{Y=1}^M G_{iY} A(kZ_Y) = - \sum_{Y=1}^M G_{iY}^* A(kZ_Y)
 \end{aligned} \quad (3.19)$$

( $i = 1 \sim N_1^{(1)}, 1 \sim N_2^{(1)}, 1 \sim N_3^{(1)}$  and  $(l, z_p)$  on AB)

where

$$G_{iY} = \bar{E}_{iY} + i\lambda_0 E_{iY}, \quad G_{iY}^* = \bar{E}_{iY} - i\lambda_0 E_{iY} \quad (3.20)$$

(b) For fluid region (III):

$$\begin{aligned}
 & -\phi^{(3)}(i) + \sum_{j=1}^{N_1^{(3)}} (\bar{E}_{ij} - \Gamma E_{ij}) \phi_i^{(3)}(j) + \sum_{j=1}^{N_2^{(3)}} [\bar{E}_{ij} \phi_2^{(3)}(j) - E_{ij} \bar{\phi}_2^{(3)}(j)] \\
 & + \sum_{j=1}^{N_3^{(3)}} \bar{E}_{ij} \phi_3^{(3)}(j) + \psi' \sum_{Y=1}^{M'} G'_{iY} A(k'Z_Y) = - \sum_{Y=1}^{M'} G'_{iY}{}^* A(k'Z_Y)
 \end{aligned} \quad (3.21)$$

( $i = 1 \sim N_1^{(3)}, 1 \sim N_2^{(3)}, 1 \sim N_3^{(3)}$  and  $(-l', z_q)$  on A'B')

where

$$G'_{iY} = \bar{E}_{iY} + i\lambda'_0 E_{iY}, \quad G'_{iY}{}^* = \bar{E}_{iY} - i\lambda'_0 E_{iY} \quad (3.22)$$

(c) For porous region (II):

$$\begin{aligned}
 & \phi^*(i) + \sum_{j=1}^{N_1^*} (\bar{E}_{ij}^* + \alpha \Gamma E_{ij}^*) \phi_i^*(j) + \sum_{j=1}^{N_2^{(1)}} \left[ \frac{1}{\beta} \bar{E}_{ij}^* \phi_2^{(1)}(j) - E_{ij}^* \bar{\phi}_2^{(1)}(j) \right] \\
 & + \sum_{j=1}^{N_3^*} \bar{E}_{ij}^* \phi_3^*(j) + \sum_{j=1}^{N_3^{(3)}} \left[ \frac{1}{\beta} \bar{E}_{ij}^* \phi_3^{(3)}(j) - E_{ij}^* \bar{\phi}_3^{(3)}(j) \right] = 0
 \end{aligned} \quad (3.23)$$

( $i = 1 \sim N_1^*, 1 \sim N_2^{(1)}, 1 \sim N_3^*, 1 \sim N_3^{(3)}$ )

and for point  $i$  on CD and C'D', that is, for  $i = 1 \sim N_2^{(1)}$  and  $i = 1 \sim N_3^{(3)}$ ,  $\phi^*(i)$  should be written as  $\frac{1}{\beta} \phi_2^{(1)}$  and  $\frac{1}{\beta} \phi_3^{(3)}$ , respectively. The points  $(l, z_p)$  and

$(-l', z_G)$  may be taken anywhere on AB and A'B', respectively.

Eq.9.2.19) (3.21) (3.23) provide  $(N_1^{(1)} + 2N_2^{(1)} + N_3^{(1)} + N_1^* + N_3^* + N_1^{(3)} + 2N_2^{(3)} + N_3^{(3)} + 2)$  linear equations with respect to the same number of unknown quantities  $\phi_1^{(1)}, \phi_2^{(1)}, \bar{\phi}_2^{(1)}, \phi_3^{(1)}; \phi_1^*, \phi_3^*; \phi_1^{(3)}, \phi_3^{(3)}, \bar{\phi}_3^{(3)}, \phi_2^{(3)}$  and  $\psi, \psi'$ . Consequently, solving these equations simultaneously, we can determine all of the unknown quantities, by which the potential values at any point in the fluid regions are calculated by means of Eq.(2.3) and the reflection and transmission coefficients are by Eq.(3.6). The surface wave profiles are provided by the real parts of the following expressions:

$$\begin{aligned} \text{From A' to C': } \zeta(j) &= -i\phi_1^{(j)} e^{i\sigma t} & ; j = N_1^{(3)} \sim 1 \\ \text{From C' to C: } \zeta(j) &= -i\beta\phi_1^*(j) e^{i\sigma t} & ; j = 1 \sim N_1^* \\ \text{From C to A: } \zeta(j) &= -i\phi_1^{(j)} e^{i\sigma t} & ; j = N_1^{(1)} \sim 1 \end{aligned} \quad (3.24)$$

Fig.3-3 is the calculated and observed reflection and transmission coefficients of permeable breakwater with 1:1.5 sloped faces and with the width  $h$  at still water surface, which is placed on the horizontal bottom of water depth  $h$ . In calculations, we took  $V = 0.5$  and  $\mu/\rho = 1.0$  for every non-dimensional frequency  $\sigma^2 h/g$ , and the numbers of the calculation points on the boundaries were  $N_1^* = 10$ ,  $N_2^{(1)} = N_3^{(3)} = 7$ ,  $N_3^* = 24$ ,  $N_1^{(1)} = N_3^{(1)} = 20$ ,  $N_3^{(1)} = N_2^{(3)} = 13$  and  $M = M' = 10$ . Observed values were measured in wave flume with length 22 m, width 1.0 m and water depth  $h = 40$  cm. The model breakwater was made by quarry stones of mean diameter 6 cm with porosity 0.43. The incident wave heights were 3 to 5 cm and the reflection coefficients were measured by Healy's method. *a*

Fig.3-4 is the one for vertical-face breakwater with width  $h$  at constant water depth  $h$ . The conditions for calculation and measurements were the same as above. It was found that the calculated results by this proposed method were entirely in agreement with those by our method of continuation of velocity potentials (1971).

As seen in Fig.3-3 and 3-4, the calculated results agree well with the observed values in tendencies, in spite of the linear dependence of the drag force on fluid velocity and of the constant coefficient  $\mu/\rho$  for all frequencies.

In reality, the drag force  $F$  to the porous material induced by the flow through breakwater is proportional to the fluid velocity for low Reynolds number and to the square of the latter for high Reynolds number, and is demonstrated in the form of  $F = au + b|u|u$  in general. And if the fluid velocity  $u$  is written as  $u = u_0 \cos \sigma t$ ,  $F$  is written as follows:

$$\begin{aligned} F &= au + b|u|u = a u_0 \cos \sigma t + \frac{8}{3\pi} b u_0^2 \left( \cos \sigma t + \frac{1}{5} \cos 3\sigma t - \frac{1}{35} \cos 5\sigma t + \dots \right) \\ &= \left( a u_0 + \frac{8}{3\pi} b u_0^2 \right) \cos \sigma t + \frac{8}{3\pi} b u_0^2 \left( \frac{1}{5} \cos 3\sigma t - \dots \right) \end{aligned}$$

Therefore, the calculated results by the drag force coefficient assumed to be linearly proportional to the fluid velocity may contain errors less than 20% of the coefficient  $b$ . These errors can be adjusted by means of the Lorentz's Principle of equivalent works, but here we do not enter into the problem.

Fig.3-5 is the calculated distribution of equi-potential lines (solid lines) and its orthogonals (broken lines) for permeable breakwater in Fig.3-3 at  $\omega t = 0^\circ, 30^\circ, 60^\circ$  and  $90^\circ$ , when the incident wave crest approaches to the breakwater.

Above method is more easily applied to the permeable seawall.

Fig.3-6 is the calculated and observed reflection coefficients of 1:1 sloped-face seawall with width  $h$  at still water level on impervious bottom of depth  $h$  in front of vertical impervious wall. Fig.3-7 is the one for vertical face seawall. The conditions for calculation and observation are the same as those for above permeable breakwater. In Fig.3-6 and 3-7, the calculated values are somewhat different from observed values, but the tendencies are in good agreement.

The better agreement between the theory and experiment on permeable breakwater and seawall shall be attained by the selection of the more appropriate values of  $V$  and  $\mu/\rho$ .

The problem on the submerged breakwater is also analyzed similarly.

Fig. 3-8 is the calculated and measured reflection and transmission coefficients for impermeable submerged breakwater with trapezoidal cross-section whose upper surface is 0.6 times the lower bottom in width and 0.3 times the water depth  $h$  in depth. (a) (b) (c) are for the cases whose bottom width are 1.0, 1.5 and 2.0 times the water depth  $h$ , respectively. The calculated and measured reflection coefficients are in good agreement, while the measured transmission coefficients are somewhat lower than those of calculated values. This seems to be due to the occurrence of higher harmonic waves induced by the propagation of waves through the shallow water depth area on the upper surface of trapezoidal cross-section.

#### IV Wave Transformation by and the Motion of Floating Cylinder

In Fig.4-1, it is assumed that a cylinder of arbitrary cross-section  $CDD'C'$  with gravity center at  $(\bar{x}_c, \bar{z}_c)$  and center of buoyancy at  $(x_b, z_b)$  in equilibrium condition is moored by spring lines  $DE$  and  $D'E'$  with spring constant  $K$  on the variable sea bottom  $B'E'EB$ , and is subjected to the incident wave of frequency  $\omega$  and small amplitude  $\zeta_0$  from the right. Then, the position of the gravity center of the cylinder  $(x_c, z_c)$  and the rotation angle  $\delta$  of the cylinder around the gravity center at any time  $t$  in motion are expressed by the complex amplitude of horizontal and vertical displacements  $X, Z$  and of the rotation angle  $\theta$  as follows:

$$x_c = \bar{x}_c + X e^{i\omega t}, \quad z_c = \bar{z}_c + Z e^{i\omega t}, \quad \delta = \theta e^{i\omega t} \quad (4.1)$$



Similarly to the previous section III, the fluid region is divided into three parts (O) (I) and (O') by the geometrical surfaces AB and A'B' at constant depth h and h', sufficiently distant from the floating body.

For the velocity potential in the form of Eq.(3.1), the potential functions for region (O) and (O'), denoted by  $\phi_0$  and  $\phi_0'$ , are demonstrated by Eq.(3.2) and (3.3) and the one for region (I) is denoted by  $\phi$

- (i) Denoting the potential functions on the boundaries of region (I) by  $\phi_1$  on AC,  $\phi_2$  on CDD'C',  $\phi_3$  on C'A' and  $\phi_4$  on B'E'EB, respectively, the boundary conditions on the free surface AC and C'A', on impervious bottom B'E'EB and on geometrical surfaces AB and A'B' are provided by Eq.(3.7)(3.11) and (3.8)(3.9), respectively.
- (ii) On the oscillating surface CDD'C', the normal derivatives of the potential function  $\phi_2$  is demonstrated by the following expression, due to the kinematical boundary condition:

$$\bar{\phi} = i\Gamma \left[ \frac{X}{\zeta_0} \frac{dZ}{ds} - \frac{Z}{\zeta_0} \frac{dX}{ds} - \frac{\Theta a}{\zeta_0} \left\{ \frac{z - \bar{z}_c}{a} \frac{dX}{ds} + \frac{Z - \bar{Z}_c}{a} \frac{dZ}{ds} \right\} \right] \quad (4.2)$$

where a is the reference length to the horizontal size of the cross-section of cylinder, for example, a is taken as half width for rectangular cylinder and as the radius for circular cylinder. (x,z) is the coordinate of the point on the surface CDD'C' and s is the length measured along CDD'C'.

- (iii) The complex amplitudes X,Z and  $\Theta$  in above expression can be demonstrated by the potential function  $\phi_2$  on the immersed surface of cylinder, taking account of the equations of motion of the cylinder as follows:

$$\begin{aligned} M \frac{d^2 x_0}{dt^2} &= P_x + F_x, & M \frac{d^2 z_0}{dt^2} &= P_z + P_s + F_z \\ I_\theta \frac{d^2 \delta}{dt^2} &= T_\theta + T_s + M_\theta \end{aligned} \quad (4.3)$$

where M is the mass of the cylinder;  $I_\theta$  is the moment of inertia around the gravity center;  $P_x, P_z, T_\theta$  are the resultant horizontal and vertical fluid forces and moment around gravity center due to the fluid pressure acting to the immersed surface;  $P_s, T_s$  are the restoring force and moment for vertical displacement and rotation of cylinder due to statical fluid pressure;  $F_x, F_z, M_\theta$  are the mooring forces and moments by the mooring lines induced by the motion of cylinder.

Indicating the fluid density by  $\rho$ , the draught in mooring condition by qh ( $1 > q > 0$ ), the mass M, the moment of inertia  $I_\theta$  and the immersed volume of the cylinder V are expressed with positive constants  $\nu_1, \nu_2$  and  $\nu_3$  as follows:

$$M = \nu_1 \rho a q h, \quad I_\theta = \nu_2 \rho (a q h)^2, \quad V = \nu_3 a q h \quad (4.4)$$

Since the fluid pressure on the immersed surface is given by  $p(j) = -i \chi$

$\phi_2(x) e^{i\omega t}$ ,  $P_x$ ,  $P_z$  and  $T_\theta$  are given as follows:

$$P_x = -i\rho g \zeta_0 e^{i\omega t} \int_S \phi_2(x, Z) dx, \quad P_z = i\rho g \zeta_0 e^{i\omega t} \int_S \phi_2(x, Z) dx$$

$$T_\theta = i\rho g \zeta_0 e^{i\omega t} \int_S \{ (x - \bar{x}_0) dx + (Z - \bar{Z}_0) dZ \} \phi_2(x, Z) \quad (4.5)$$

where integrations are taken along the surface CDD'C'.

Denoting the length of water line as  $2l_0$ ,  $P_s$  and  $T_s$  are given as

$$P_s = -2\rho g l_0 Z e^{i\omega t}, \quad T_s = -\rho g \Gamma \left\{ \frac{2}{3} \frac{l_0^3}{V} - (\bar{Z}_0 - Z) \right\} \Theta e^{i\omega t} \quad (4.6)$$

For simplicity, we assume that the cross-section of the cylinder and the mooring conditions are symmetrical with respect to the vertical line through the gravity center. Then, taking the angle of mooring line with horizontal as  $\beta$  and the mooring points on the cylinder as  $(a_c, b_c)$  and  $(-a_c, b_c)$ , the mooring forces and moments to the cylinder  $F_x$ ,  $F_z$  and  $M_\theta$  are expressed as follows:

$$F_x = -2K(X - S\Theta) \cos^2\beta \cdot e^{i\omega t}, \quad F_z = -2K \sin^2\beta \cdot e^{i\omega t}$$

$$M_\theta = 2KS(X - S\Theta) \cos^2\beta \cdot e^{i\omega t} \quad \text{where} \quad S = b_0 - \bar{z}_c - (a_0 - \bar{x}_0) \tan\beta \quad (4.7)$$

Substituting Eq. (4.1) (4.4) (4.5) (4.6) and (4.7) into Eq. (4.3), it follows that  $X$ ,  $Z$  and  $\Theta$  are expressed by  $\phi_2(x, z)$  as

$$\frac{X}{\zeta_0} = \frac{i}{\gamma} \int_S \phi_2(x, Z) \left\{ k_{x0} \frac{x - \bar{x}_0}{a} \frac{dx}{a} + (k_{z0} \frac{Z - \bar{Z}_0}{a} - \alpha_3) \frac{dZ}{a} \right\} \quad (4.8)$$

$$\frac{Z}{\zeta_0} = \frac{i}{\alpha_2} \int_S \phi_2(x, Z) \frac{dZ}{a} \quad (4.9)$$

$$\frac{\Theta a}{\zeta_0} = \frac{i}{\gamma} \int_S \phi_2(x, Z) \left\{ \alpha_1 \frac{x - \bar{x}_0}{a} \frac{dx}{a} + \left( \alpha_1 \frac{Z - \bar{Z}_0}{a} - k_{z0} \right) \frac{dZ}{a} \right\} \quad (4.10)$$

where

$$\gamma = \alpha_1 \alpha_3 - k_{z0}^2, \quad \alpha_1 = k_{xz} - \nu_1 \frac{qh}{h_0} \Gamma$$

$$\alpha_2 = k_{zz} - \nu_1 \frac{qh}{h_0} \Gamma + \frac{2l_0}{a}, \quad \alpha_3 = k_{\theta\theta} - \nu_2 \frac{(qh)^3}{ah_0} \Gamma + \frac{2}{3} \left( \frac{l_0}{a} \right)^3 - \nu_3 \frac{qh}{a} \frac{\bar{Z}_0 - Z_b}{a}$$

$$k_{xx} = \frac{2K}{\rho g a} \cos^2\beta, \quad k_{zz} = \frac{2K}{\rho g a} \sin^2\beta, \quad k_{\theta\theta} = \frac{2KS^2}{\rho g a^3} \cos^2\beta, \quad (4.11)$$

$$k_{x0} = \frac{2KS}{\rho g a^2} \cos^2\beta$$

(iv) Introducing Eq. (4.8) (4.9) (4.10) into Eq. (4.2),  $\bar{\phi}_2$  on the immersed surface of cylinder is written by  $\phi_2$  as follows:

$$\bar{\phi}_2(x, z) = \Gamma \int_S \phi_2(u, v) dF(z, z; u, v) \quad (4.12)$$

where

$$dF(x, z; u, v) = \left[ \left( \frac{1}{\alpha_2} + \frac{\alpha_1}{\gamma} \frac{u - \bar{x}_0}{a} \frac{x - \bar{x}_0}{a} \right) \frac{dx}{ds} - \frac{1}{\gamma} \left( k_{x\theta} - \frac{z - \bar{z}_0}{a} \right) \cdot \frac{u - \bar{x}_0 dz}{a} \frac{du}{a} + \frac{1}{\gamma} \left[ \left( \alpha_1 \frac{v - \bar{z}_0}{a} - k_{x\theta} \right) \frac{x - \bar{x}_0}{a} \frac{dx}{ds} + \left( \alpha_3 - k_{x\theta} \frac{z - \bar{z}_0}{a} - \left( k_{x\theta} - \alpha_1 \frac{z - \bar{z}_0}{a} \right) \frac{v - \bar{z}_0}{a} \right) \frac{dv}{a} \right] \quad (4.13)$$

where  $(x, z)$  and  $(u, v)$  are the coordinates of the points on the immersed surface. Indicating the calculation points on the surface as  $(\xi_j, \eta_j)$  and  $(\xi_m, \eta_m)$ , corresponding to  $(x, z)$  and  $(u, v)$ , Eq. (4.12) is written as follows:

$$\bar{\phi}_2(x, z) = \Gamma \sum_{m=1}^{N_2} \phi_2(m) dF(j, m) \quad (4.14)$$

(v) Similarly to the preceding section, applying Eq. (3.7) (3.11) (3.8) (3.9) and (4.14) to the Green's identity formula (2.4) for fluid region (I), we have the following linear equations with respect to the potential functions  $\phi$  on the boundaries and  $\psi, \psi'$ :

$$\begin{aligned} & -\phi(i) + \sum_{j=1}^{N_1} (\bar{E}_{ij} - \Gamma E_{ij}) \phi_j(j) + \sum_{m=1}^{N_2} \sum_{j=1}^{N_2} [\delta_{jm} \bar{E}_{ij} - \Gamma E_{ij} dF(j, m)] \phi_2(m) \\ & + \sum_{j=1}^{N_3} (\bar{E}_{ij} - \Gamma E_{ij}) \phi_3(j) + \sum_{j=1}^{N_4} \bar{E}_{ij} \phi_4(j) + \psi \sum_{\gamma=1}^M G_{i\gamma} A(kZ_\gamma) + \psi' \sum_{\gamma=1}^{M'} G'_{i\gamma} A(k'Z'_\gamma) \\ & = - \sum_{\gamma=1}^M G_{i\gamma}^* A(kZ_\gamma) \quad \text{where } \delta_{jm} = 0 \text{ ( } j \neq m \text{ )} = 1 \text{ ( } j = m \text{ )} \end{aligned} \quad (4.15)$$

(  $i = 1 \sim N_1, 1 \sim N_2, 1 \sim N_3, 1 \sim N_4$  and  $(\ell, z_p)$  on AB,  $(-\ell', z_q)$  on A'B' )

Solving the equations, we can obtain all of the boundary-values of potential function of region (I) and the reflection and transmission coefficients, similarly to the section III. Then, the amplitudes of motion of cylinder are calculated by Eq. (4.8) (4.9) (4.10) and also the mooring force F to the wave-side mooring line DE is calculated as follows:

$$\frac{F}{\zeta_0 K} = \left[ \frac{X}{\zeta_0} + \frac{Z}{\zeta_0} \tan \beta - \frac{\theta}{\zeta_0} \frac{a}{a} \frac{S}{a} \right] \cos \beta e^{i\omega t} \quad (4.16)$$

The mooring force to the lee-side line D'E' is demonstrated by replacing  $\beta$  by  $-\beta$  in above expression.

As an example, we consider the case when a circular cylinder of uniform density 0.584 with diameter  $D = 32$  cm is moored by spring lines of spring constant  $K = 0.227 \rho g a$  with mooring angle  $\beta = 33^\circ$  in water of constant depth  $h = 35$  cm and the gravity center of the cylinder is 4.0 cm below still water level in equilibrium condition. In this case,  $D (= 2a) = 0.914 h$ , the draught is  $0.67 h$  ( $q = 0.67$ ), the mooring points on the cylinder are  $(\pm 0.486 h, -0.114 h)$ , and  $V_1 = 1.467$ ,  $V_2 = 0.670$  and  $V_3 = 1.646$ .

Fig.4-2 is the calculated (solid line) and measured (open circles) transmission coefficients with respect to the non-dimensional frequency or to the ratio of diameter to wave length  $D/L$ . Experiments were carried out in wave flume with water depth 35 cm, length 22 m and width 1.0 m. The figure shows that the calculated and measured values are in good agreement. Moreover, it shows an interesting fact that the incident wave is perfectly intercepted even by floating cylinder, if the frequency  $\delta^2 h/g$  is 0.42 and 1.74, that is,  $D/L$  is 0.10 and 0.26. Fig.4-3 is the calculated reflection coefficient and amplitudes of motion of cylinder.

#### V Conclusions

It is clear that the proposed method provides a convenient and simplified analyses for two-dimensional boundary-value problems of small amplitude waves. And, if the difficulties arising in solving simultaneous equations of so many unknown quantities were overcome, this method is extended directly to the problem of three-dimensional waves and also to the finite amplitude wave problems by means of perturbation method.

#### References

- Ijima, T., Y. Eguchi and A. Kobayashi (1971): " Permeable Breakwater and Seawall ", Proc. 18th Japanese Conf. Coast. Eng. J.S.C.E.
- Ijima, T., Y. Tabuchi and Y. Yumura (1972): " Scattering of Surface waves and the Motion of Rectangular Body in Waves of Finite Water Depth ", Proc. J.S.C.E. No.202
- Ijima, T. and C.R. Chou (1976): " Analyses of Two-Dimensional Wave Problems by Means of Green's Identity Formula ", Proc. J.S.C.E. No.252
- Ijima, T. and C.R. Chou (1976): " Analyses of Boundary-Value Problems by Means of Green's Identity Formula for Two-Dimensional Waves of Finite Water Depth ", Memorirs of the Faculty of Engineering, Kyushu University, Vol.35, No.3

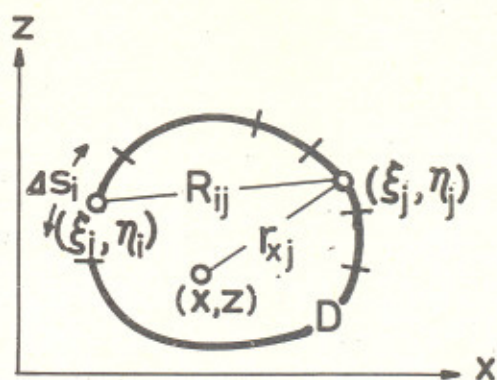
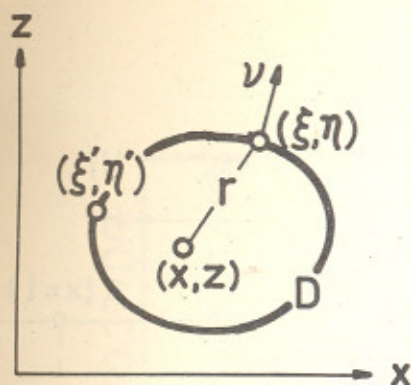


Fig.2-1 Definition Sketch Fig.2-2 Definition Sketch

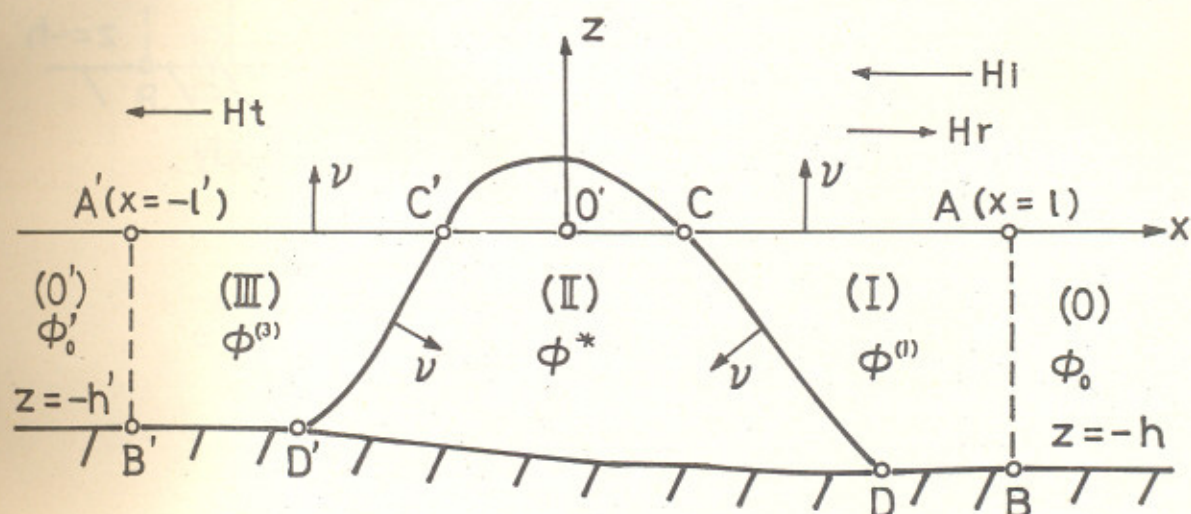


Fig.3-1 Definitions for Fluid Regions  
(Permeable Breakwater)

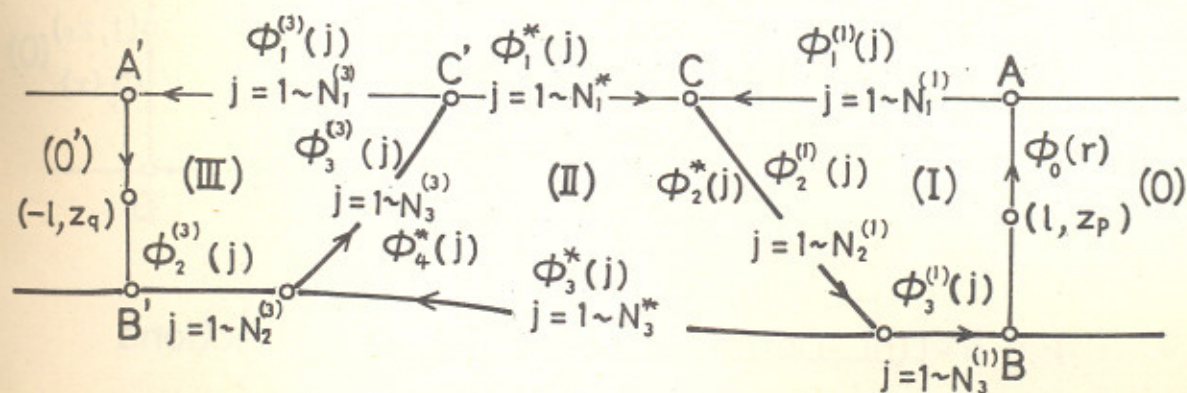


Fig.3-2 Definitions for Potential Functions

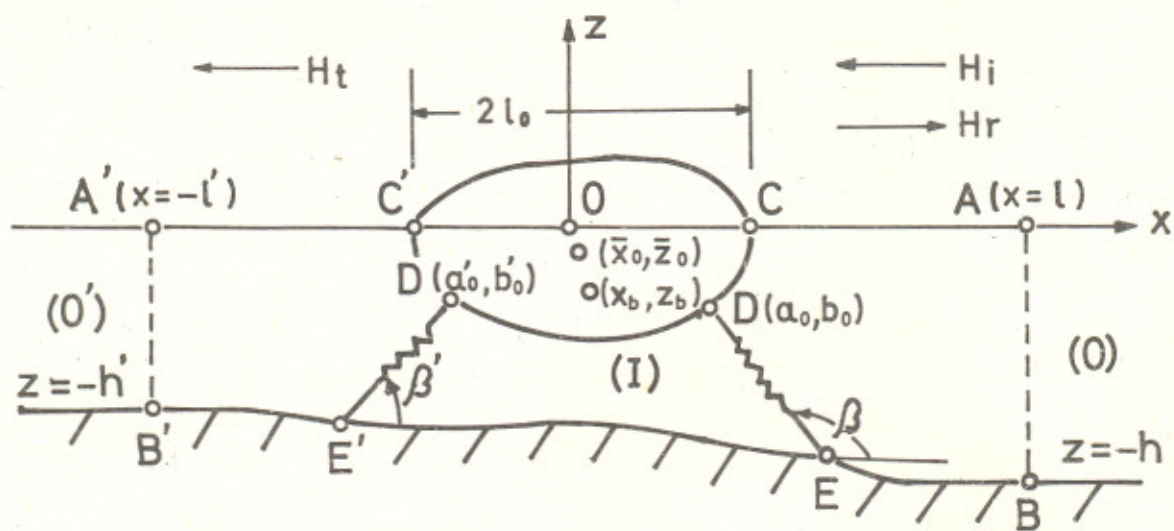


Fig. 4-1(a) Definition of Floating Body

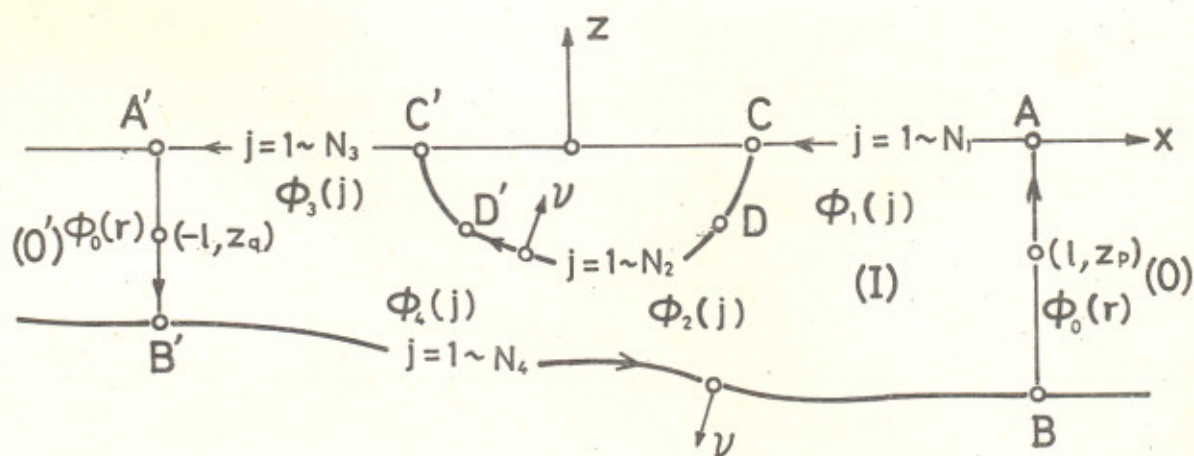


Fig. 4-1(b) Definition of Potential Functions

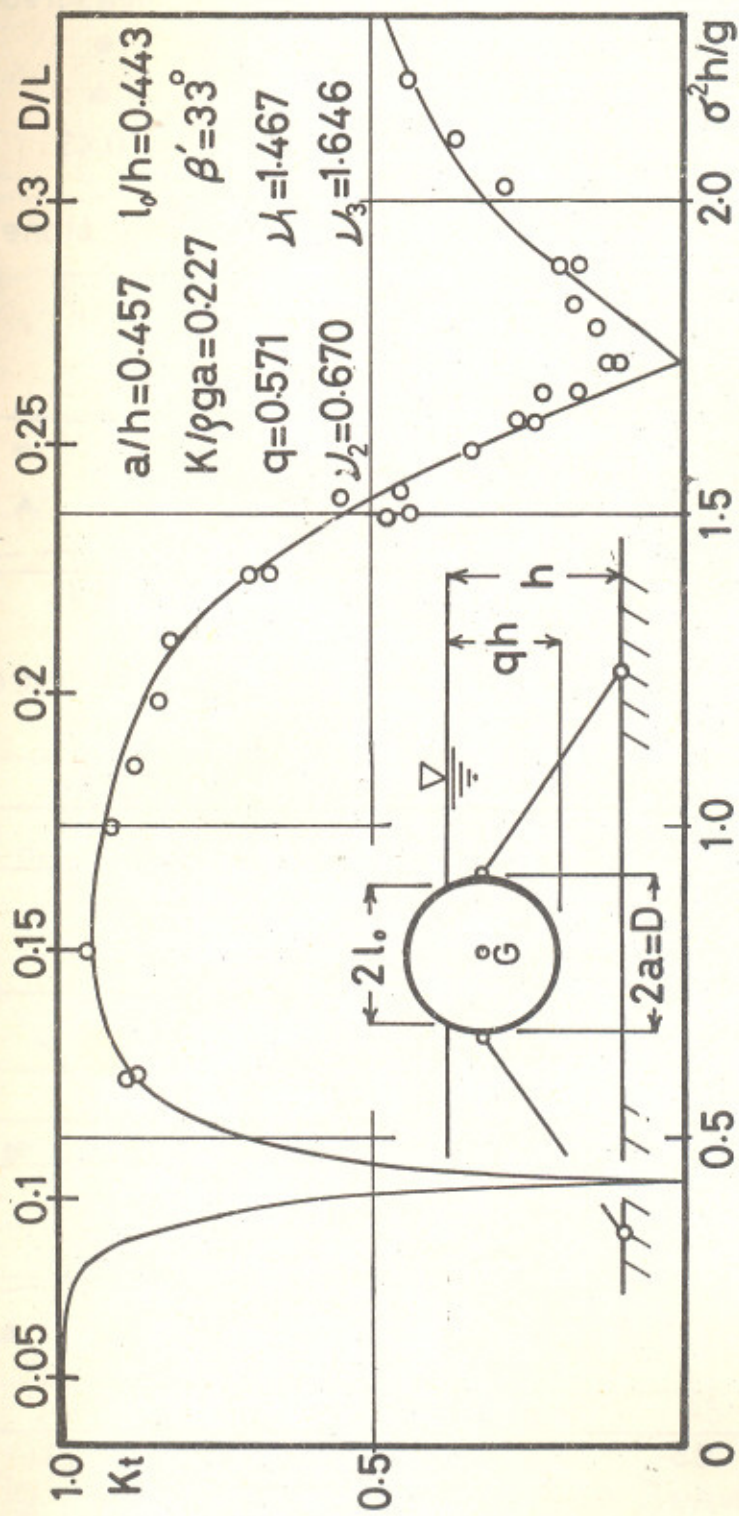


Fig. 4-2 Transmission coefficient of moored floating cylinder

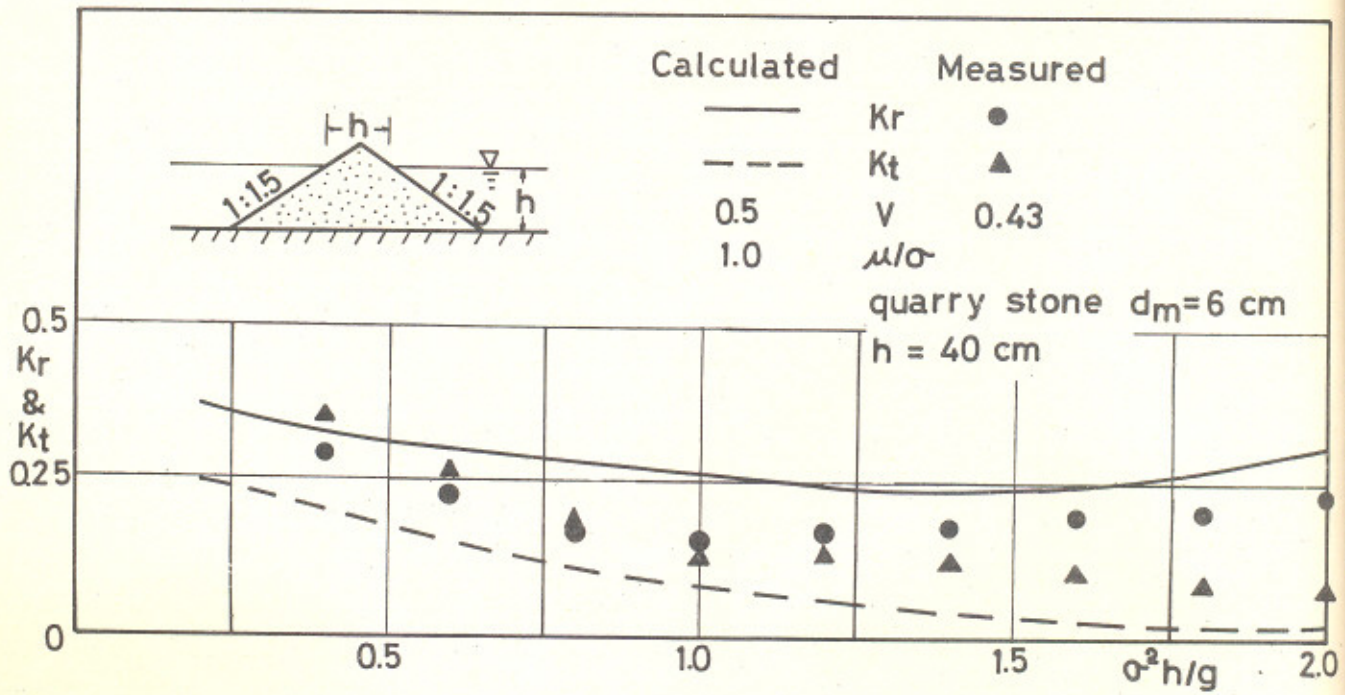


Fig.3-3  $K_r$  and  $K_t$  for Breakwater with Sloped Faces

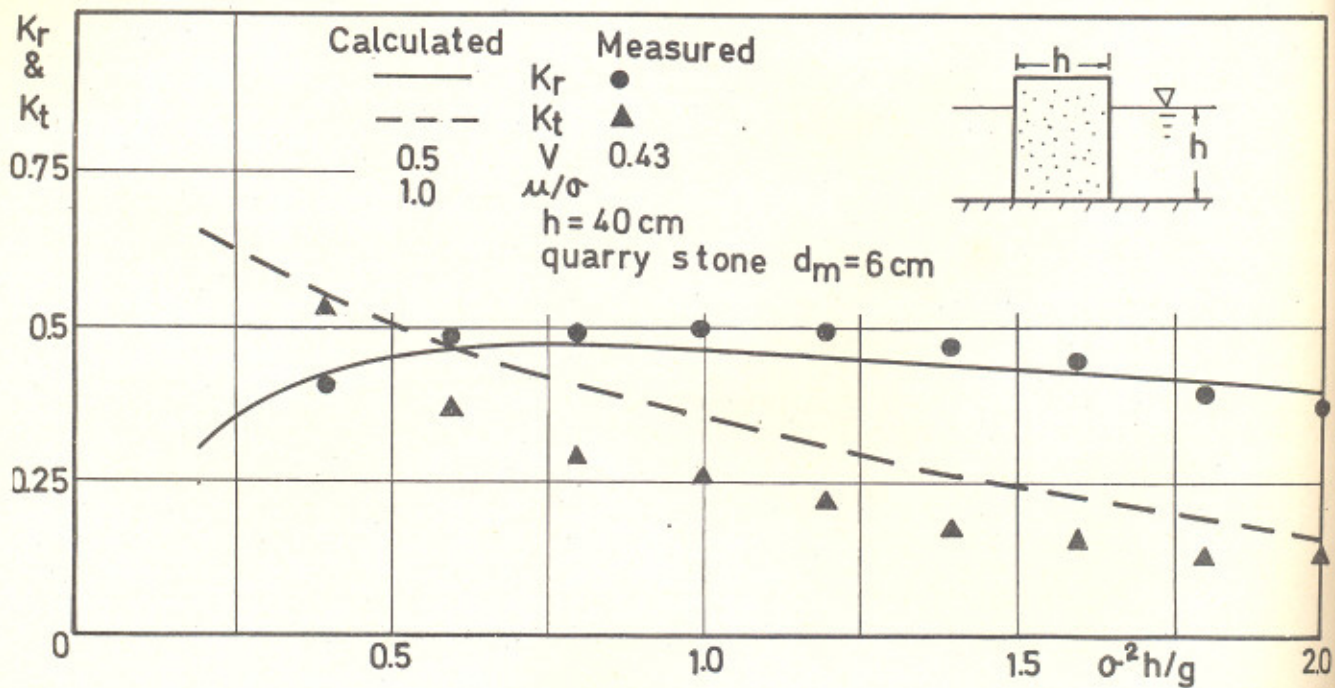


Fig.3-4  $K_r$  and  $K_t$  for Vertical-Face Breakwater



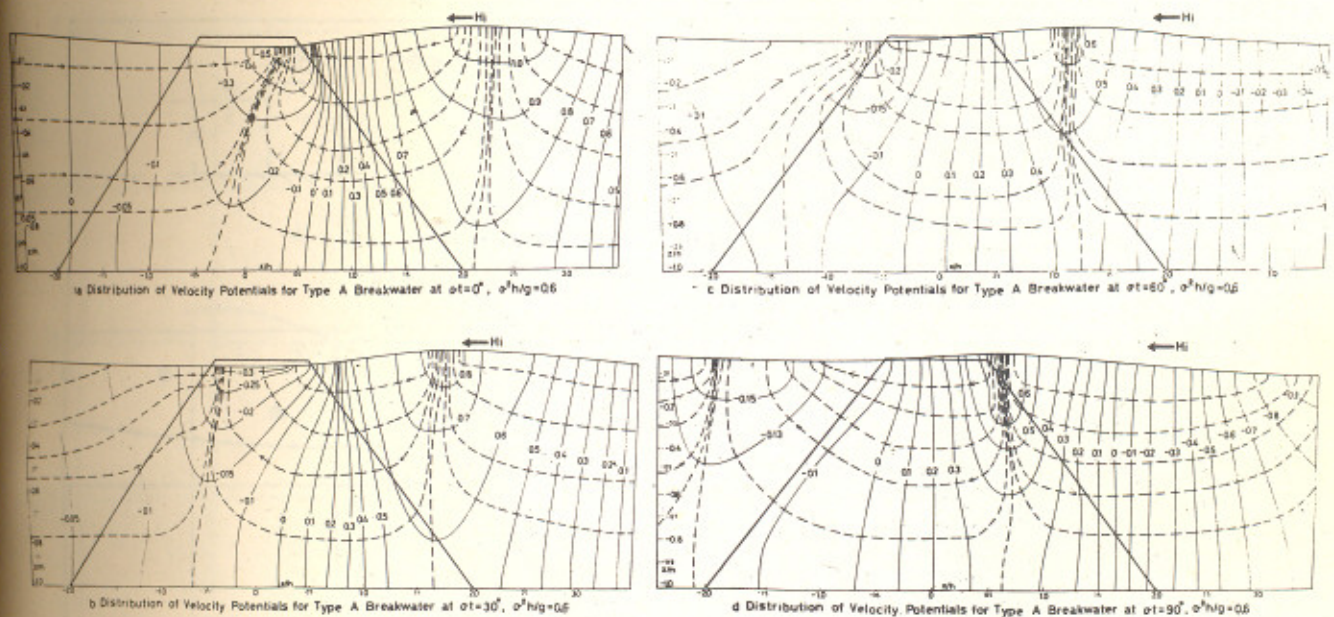


Fig. 3-5

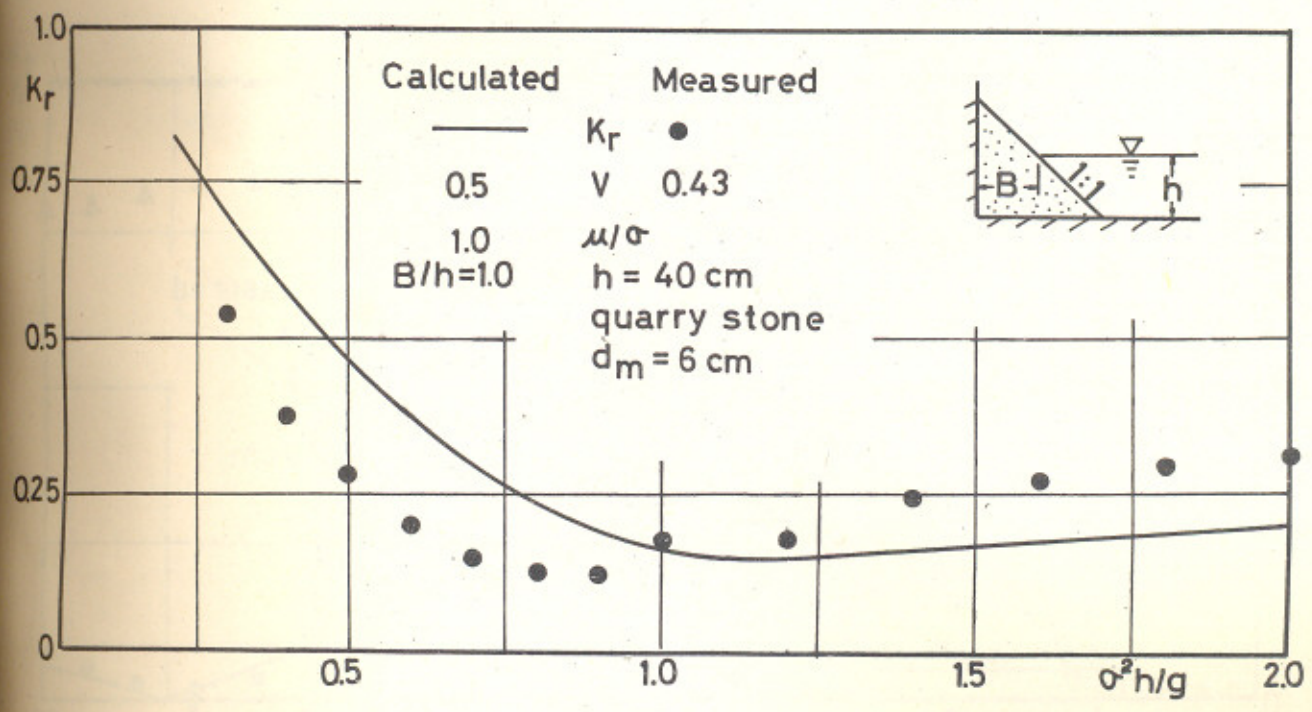


Fig. 3-6  $K_r$  for Sloped-Face Seawall

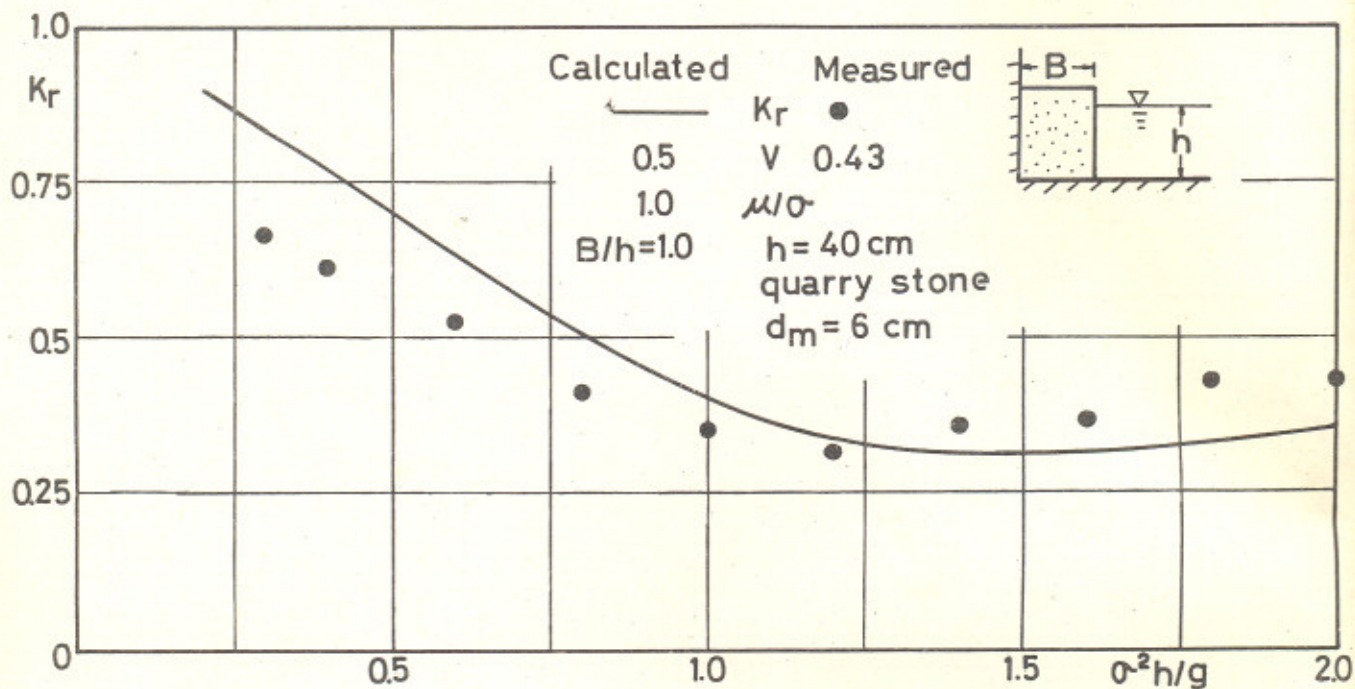


Fig.3-7  $K_r$  for Vertical-Face Seawall

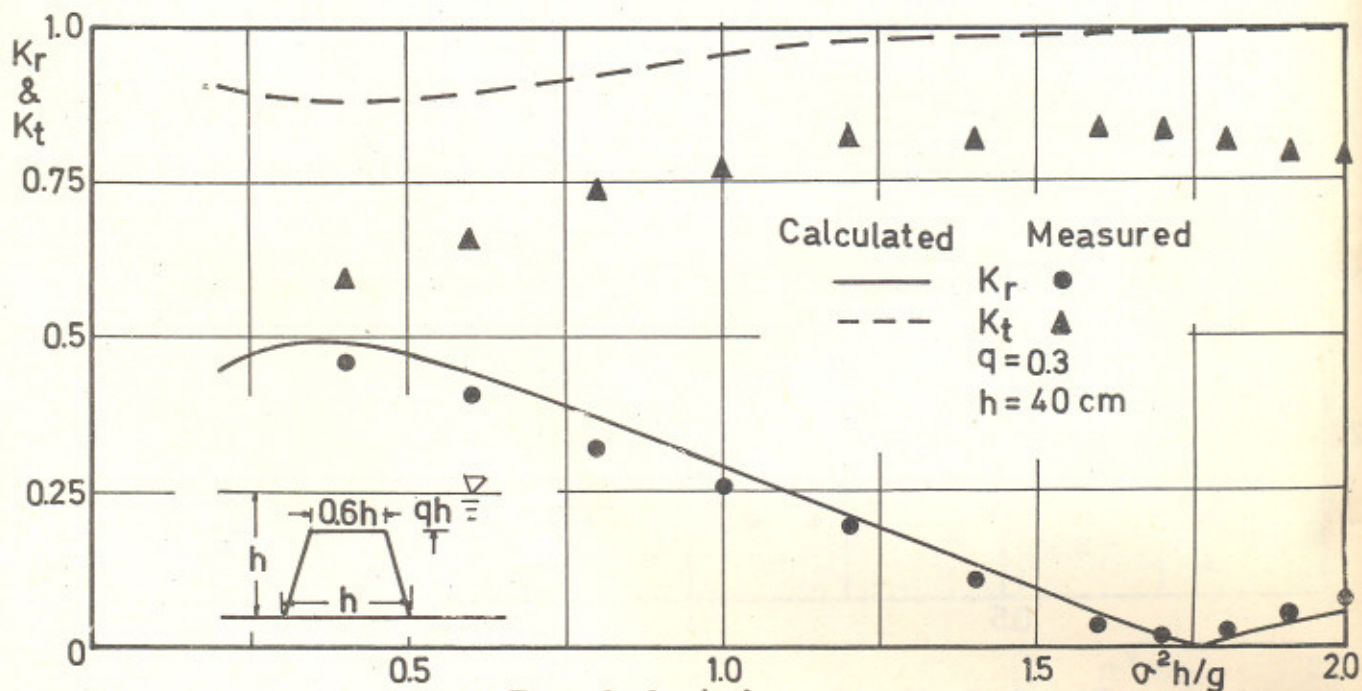


Fig.3-8 (a)

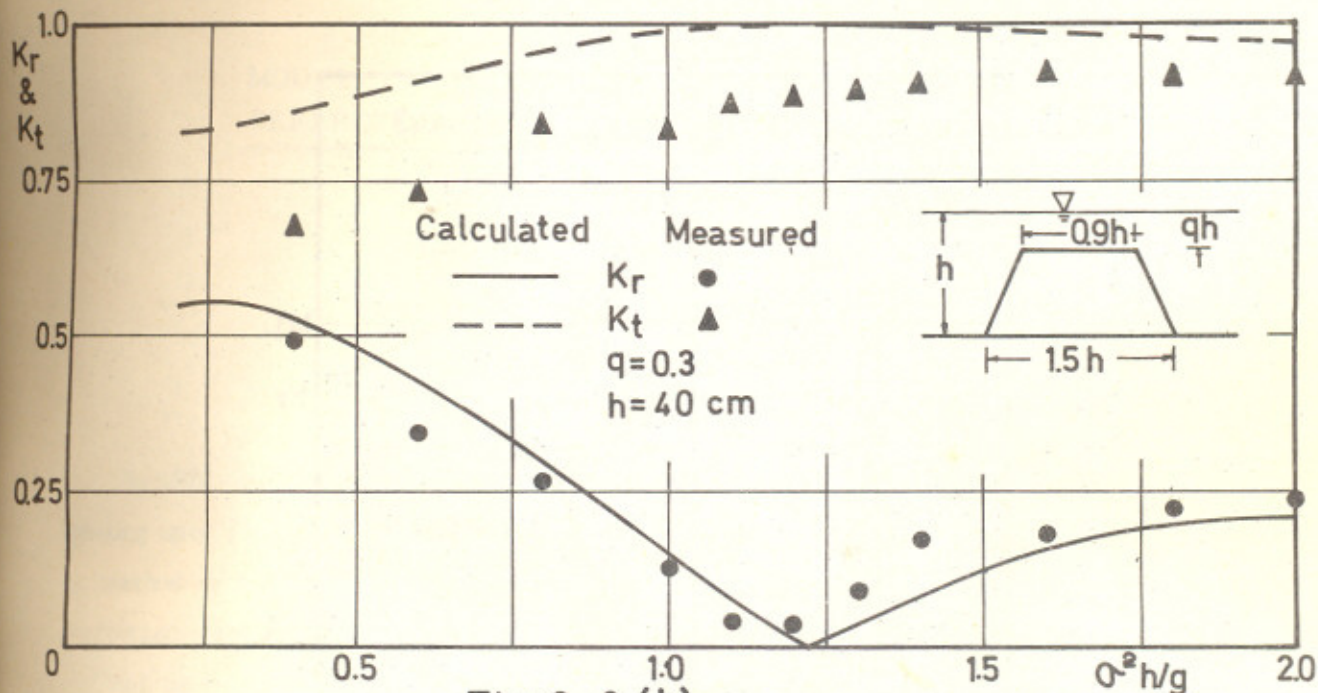


Fig. 3-8 (b)

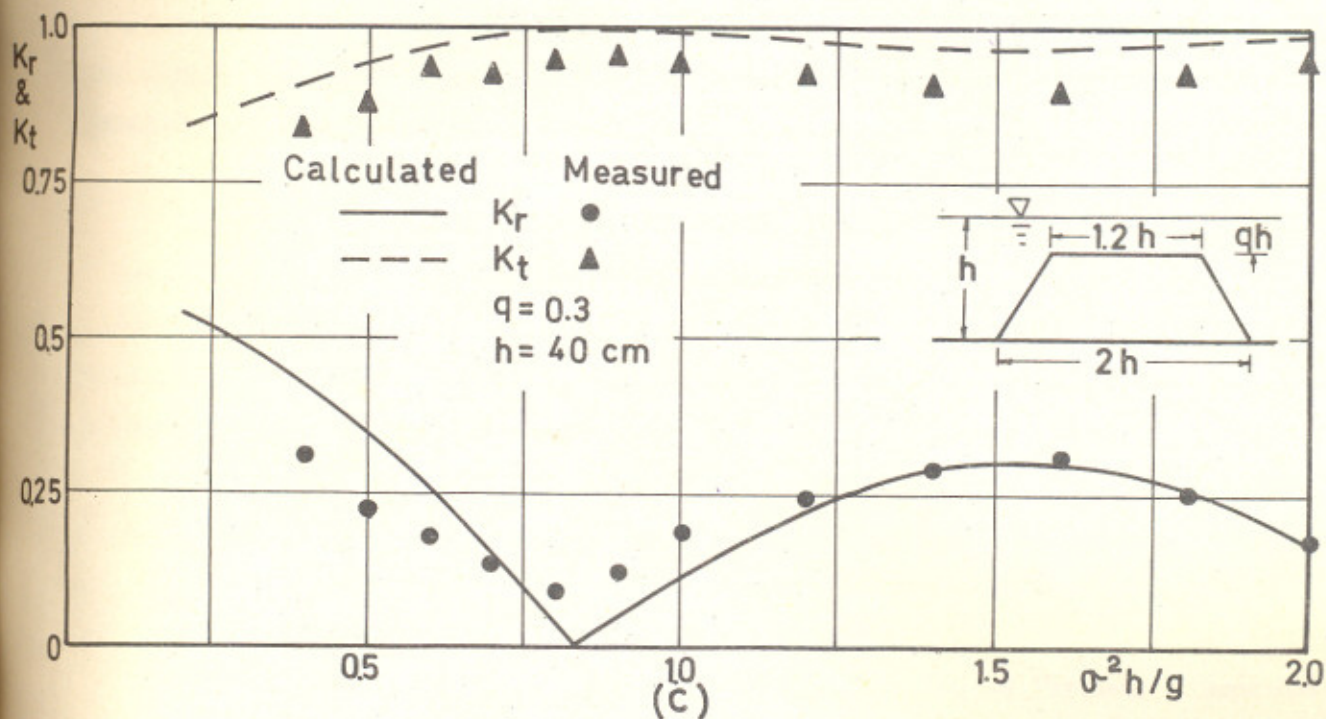


Fig. 3-8  $K_r$  and  $K_t$  for Impermeable Submerged Breakwater

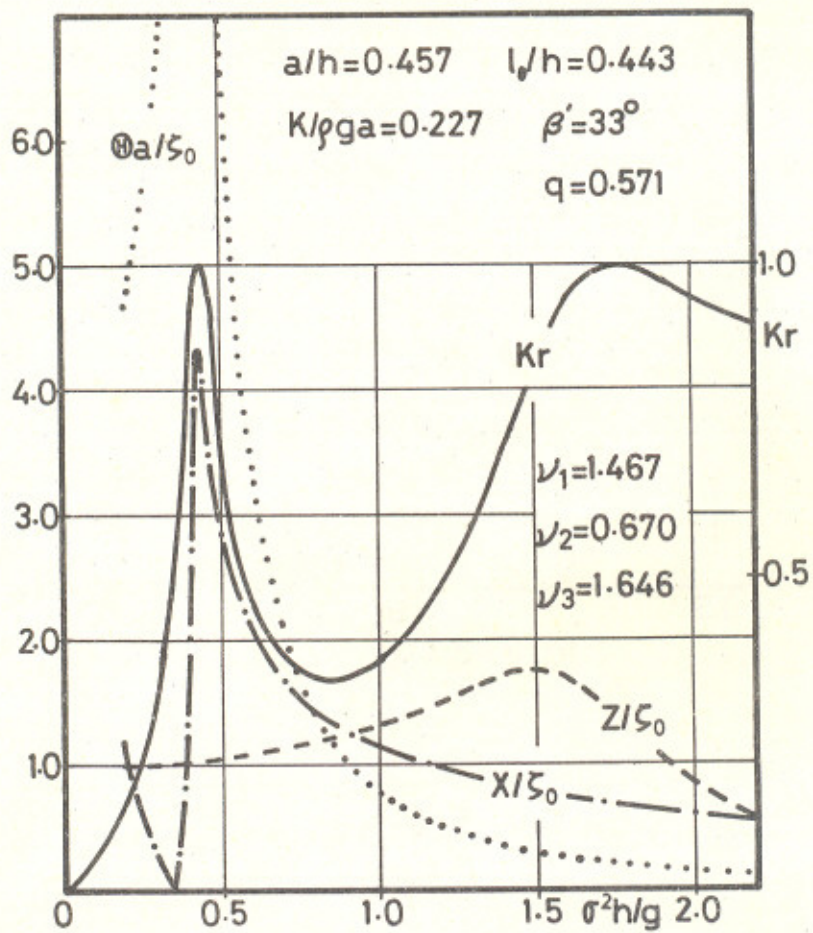


Fig. 4-3 Amplitude of motions and Reflection coefficient